International Journal of Quantum Information
Vol. 12, No. 2 (2014) 1461015 (9 pages)

DOI: 10.1142/S0219749914610152

World Scientific
www.worldscientific.com

About the use of fidelity in continuous variable systems

Antonio Mandarino* and Matteo Bina

Dipartimento di Fisica dell'Università degli Studi di Milano, 20133 Milan, Italy
**antonio.mandarino@unimi.it*

Stefano Olivares and Matteo G. A. Paris

Dipartimento di Fisica, Università degli Studi di Milano, I-20133 Milan, Italy

CNISM, UdR Milano, I-20133 Milan, Italy

Received 14 January 2014
Accepted 16 January 2014
Published 6 May 2014

We present examples of continuous variable (CV) states having high fidelity to a given target, say $F > 0.9$ or $F > 0.99$, and still showing striking differences in their physical properties, including classical and quantum states within the set, separable and entangled ones, or nearly Gaussian and strongly non-Gaussian ones. We also show that the phenomenon persists also when one imposes additional constraints on the energy or the squeezing fraction of the states, thus generally questioning the use of fidelity to assess properties of CV systems without a tomographic set of additional constraints.

Keywords: Fidelity; continuous variable systems.

1. Introduction

Fidelity[1] is a widely adopted figure of merit to compare quantum states and to assess generation and characterization schemes of interest for quantum technology, e.g. quantum interferometry.[2–4] Fidelity between the two states ρ_1 and ρ_2 is defined as follows:

$$F(\rho_1, \rho_2) = (\mathrm{Tr}\sqrt{\sqrt{\rho_1}\rho_2\sqrt{\rho_1}})^2. \tag{1}$$

The Bures distance may be expressed in terms of fidelity:

$$D_B(\rho_1, \rho_2) = \sqrt{2[1 - \sqrt{F(\rho_1, \rho_2)}]}, \tag{2}$$

*Corresponding author.

which also provides an upper and lower bounds to the trace distance[5]:

$$1 - \sqrt{F(\rho_1, \rho_2)} \leq \frac{1}{2}||\rho_1 - \rho_2||_1 \leq \sqrt{1 - F(\rho_1, \rho_2)}. \tag{3}$$

Fidelity is bounded to the interval $[0, 1]$, and values above a given threshold close to unit, say, 0.9 or 0.99 are usually considered as a sign that the two states are close to each other, and so share nearly identical properties. The first statement is certainly true, as it follows from the links between the fidelity and the Bures and trace distances, whereas the second one may not be justified, or even wrong in some cases.[6–8] The main purpose of this paper is to continue and extend the analysis of Ref. 9, providing examples, in continuous variable (CV) systems, where high values of fidelity are achieved by pair of states with considerably different physical properties, as for example separable and entangled states, classical and non-classical ones or, going beyond the Gaussian sector, states with very different values of non-Gaussianity.

The paper is structured as follows. In Sec. 2, we deal with single-mode Gaussian states and analyze the drawbacks of the use of fidelity in assessing their quantumness, defined either in terms of Glauber P-functions or via the Fano factor. In Sec. 3, we focus on two-mode states and show how high values of fidelity may be achieved by separable and entangled states or by states with very different values of non-Gaussianity. Section 4 closes the paper with some concluding remarks.

2. Single-Mode Gaussian State

Here we consider a generic single-mode Gaussian state that is a displaced squeezed thermal state (DSTS_1):

$$\rho(x, r, n_T) = D(x)S(r)\nu_{\mathrm{th}}(n_T)S^\dagger(r)D^\dagger(x), \tag{4}$$

where $S(r) = \exp\{\frac{1}{2}r(\hat{a}^{\dagger 2} - \hat{a}^2)\}$ and $D(x) = \exp\{x(\hat{a}^\dagger - \hat{a})\}$, with $r, x \in \mathbb{R}$, are the single-mode squeezing and the displacement operators, respectively, $\nu_{\mathrm{th}}(n_T)$ is a thermal state with mean photon number n_T. The covariance matrix (CM) of the state in (4) is diagonal $\sigma = \mathrm{diag}(a, b)$ with $a = (n_T + \frac{1}{2})e^{2r}$, $b = (n_T + \frac{1}{2})e^{-2r}$. A suitable parametrization for DSTS_1 may be obtained using the coherent amplitude x, the average photon number of the squeezed thermal kernel $\rho(0, r, n_T)$, i.e. $N = n_T + n_S + 2n_T n_S$, with $n_S = \sinh^2 r$ the number of squeezed photons, and the squeezing fraction $\beta \equiv n_s/N \in [0, 1]$. The total average photon number of DSTS_1 (from now on the *energy*) is given by $\langle a^\dagger a\rangle \equiv \langle n\rangle = x^2 + N$ and the thermal and squeezing component may be expressed as:

$$n_T = \frac{(1-\beta)N}{1 + 2\beta N} \quad \text{and} \quad n_S = \beta N, \tag{5}$$

respectively.

The non-classicality of a DSTS_1 may be detected using the Fano factor defined as the ratio of the variance of photon number over the mean photon number[14]:

$$R = \frac{\langle n^2 \rangle - \langle n \rangle^2}{\langle n \rangle}. \tag{6}$$

One has $R = 1$ for coherent states, while a smaller value is a sufficient condition for non-classicality, since no state endowed with a positive Glauber P-function may be sub-Poissonian. The fidelity between two single-mode Gaussian states $\rho_k(x_k, r_k, n_{T,k})$, with $k = 1, 2$, may be written as[11,12]:

$$F_{N\beta x} = \frac{\exp\{-\frac{1}{2}(\mathbf{X_1} - \mathbf{X_2})^T(\sigma_1 + \sigma_2)^{-1}(\mathbf{X_1} - \mathbf{X_2})\}}{\sqrt{\Delta + \delta} - \sqrt{\delta}}, \tag{7}$$

where σ_1 and σ_2 are the corresponding covariance matrices, $\Delta = \det[\sigma_1 + \sigma_2]$, $\delta = 4\prod_{k=1}^{2}(\det[\sigma_k] - \frac{1}{4})$, and where $\mathbf{X_k} = (x_k, 0)$. In Fig. 1 (left panel) we show DSTS_1 as points in the space parametrized by N, β and x: the red region corresponds to sub-Poissonian states, whereas the blue one contains states having fidelity $F_{N\beta x} > 0.99$ to a DSTS_1 target with the same value of N, that is the average photon number of the squeezed thermal kernel, and $\beta = 0.5$ and $x = 0.5$ (dashed line in the figure). For the sake of clarity, we report in the right panel of Fig. 1(b) a section of the

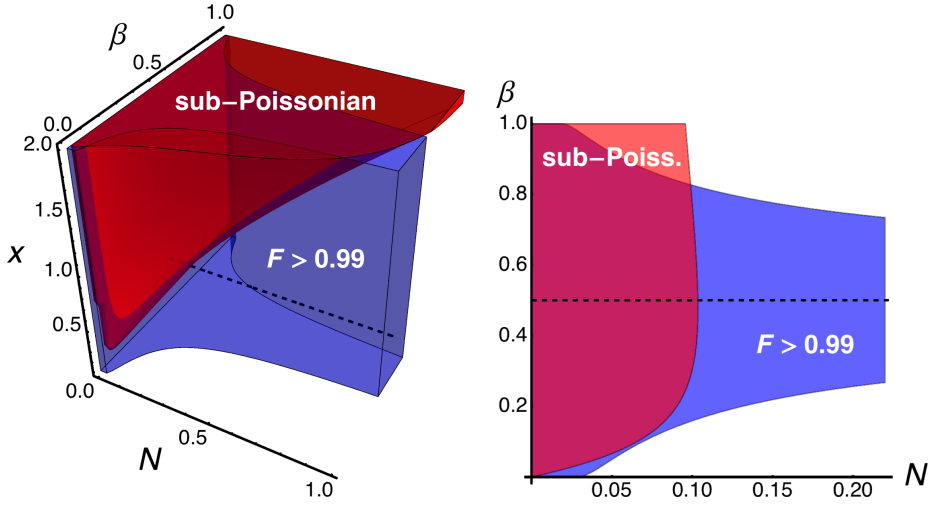

Fig. 1. (Color online) Fidelity and sub-Poissonianity. (Left panel) The red region contains the sub-Poissonian DSTS_1 whereas the blue one refers to states with fidelity $F_{N\beta x} > 0.99$ to a target DSTS_1 with the same N and fixed $\beta = 0.5$ and $x = 0.5$ (black-dashed line). (Right panel) Section of the plot of the left panel in correspondence of $x = 0.5$. Note that here N is not the total energy, but the average photon number of the squeezed thermal kernel (see text for details).

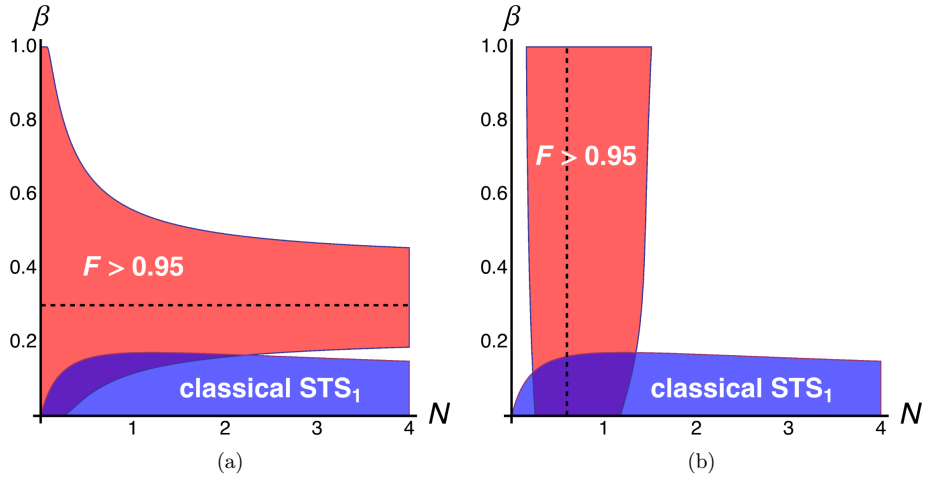

Fig. 2. (Color online) Fidelity and non-classicality. Classicality regions for STS_1 (blue regions) and regions of states having fidelity $F_{N\beta} > 0.95$ (red regions) to the set of target states (black-dashed line) as functions of N and β. The target states have fixed $\beta = 0.3$ (left panel) or fixed $N = 0.6$ (right panel).

left panel by fixing $x = 0.5$. As it is apparent from the plot, this set includes both sub-Poissonian and super-Poissonian states, independently of the nature of the target state. Overall, this means that fidelity cannot be used to assess the sub-Poissonian character of $DSTS_1$ even when quite strict constraints are imposed on the set of considered states (in this case the parameter N).

The most general way to assess the quantum properties of a single-mode state is to study whether the Glauber P-function is singular or not.[10] Let us focus attention to single-mode squeezed thermal states, i.e. let us set $x = 0$ in Eq. (4), and analyze the relationships between non-classicality and fidelity. In the left panel of Fig. 2 we show the region of classicality for STS_1 states as a function of the total energy $\langle n \rangle = N$ and the squeezing fraction β together with the region of states having a fidelity $F_{N\beta} > 0.95$ to the set of non-classical states with fixed squeezing fraction $\beta = 0.3$. The right panel of Fig. 2 displays the region of classical states together with the region of states having a fidelity $F_{N\beta} > 0.95$ to the set of states with fixed energy $N = 0.6$. In both cases the areas have a non-zero overlap and cross the non-classical boundary, such that fidelity cannot be used as unique figure of merit in order to assess quantumness. To summarize: we have strong evidence that fidelity should not be used in benchmarking the generation of quantum resources, even when attention is focused on states with quite stringent physical constraints, as fixed energy or squeezing. Only after a full tomographic reconstruction of the state one obtains a suitable set of physical constraints to properly decrease the volume of states having a given value of fidelity to the target or the set of target states.[13]

3. Two-Mode States

Let us now consider two-mode squeezed thermal states, expressed by the density operator:

$$\rho = S_2(r)\nu_{\rm th}(n_{T1}) \otimes \nu_{\rm th}(n_{T2})S_2^\dagger(r), \tag{8}$$

where $S_2(r) = \exp\{r(\hat{a}^\dagger\hat{b}^\dagger - \hat{a}\hat{b})\}$, with $r \in \mathbb{R}$, is the two-mode squeezing operator and n_{Tk} $(k = 1, 2)$ are the mean thermal photon numbers. The states in Eq. (8) are Gaussian, assuming their 4×4 CM is given by:

$$\sigma = \frac{1}{2}\begin{pmatrix} A\mathbb{I}_2 & C\hat{\sigma}_z \\ C\hat{\sigma}_z & B\mathbb{I}_2 \end{pmatrix}, \tag{9}$$

where $\mathbb{I}_2$ is the 2×2 identity matrix, $\hat{\sigma}_z$ is the Pauli matrix and:

$$A \equiv A(\beta, \gamma, N) = 1 + \frac{2\gamma(1-\beta)N + \beta N(1+N)}{1+\beta N}, \tag{10a}$$

$$B \equiv B(\beta, \gamma, N) = 1 + \frac{2(1-\gamma)(1-\beta)N + \beta N(1+N)}{1+\beta N}, \tag{10b}$$

$$C \equiv C(\beta, \gamma, N) = \frac{(1+N)\sqrt{\beta N(2+\beta N)}}{1+\beta N}, \tag{10c}$$

where now $N \equiv 2n_S + (n_{T1} + n_{T2})(1 + 2n_S)$ is the total energy, $\beta \equiv 2n_S/N$ is the fraction of squeezed photons, and $\gamma \equiv n_{T1}/(n_{T1} + n_{T2})$ is the fraction of single-mode thermal photons.

A way to quantify the nonclassicality of a two-mode Gaussian state is in terms of the amount of entanglement. Entanglement may be detected and quantified in terms of negativity of the partial transposed density matrix. In terms of the so-called symplectic eigenvalues[15]:

$$\tilde{d}_\pm = \sqrt{\frac{\tilde{\Delta}(\sigma) \pm \sqrt{\tilde{\Delta}(\sigma)^2 - 4I_4}}{2}}, \tag{11}$$

where we introduced the local symplectic invariants $I_1 = \det[A]$, $I_2 = \det[B]$, $I_3 = \det[C]$ and $I_4 = \det[\sigma]$, a two-mode squeezed thermal state is separable iff $\tilde{d}_- \geq \frac{1}{2}$. The fidelity between two-mode Gaussian states of the type (8) reads[16,17]:

$$F_{N\beta\gamma} = \frac{(\sqrt{X} + \sqrt{X-1})^2}{\sqrt{\det[\sigma_1 + \sigma_2]}}, \tag{12}$$

where $X = 2\sqrt{E_1} + 2\sqrt{E_2} + \frac{1}{2}$ and

$$E_1 = \frac{\det[\Omega\sigma_1\Omega\sigma_2] - \frac{1}{4}}{\det[\sigma_1 + \sigma_2]} \quad \text{and} \quad E_2 = \frac{\det[\sigma_1 + \frac{i}{2}\Omega]\det[\sigma_2 + \frac{i}{2}\Omega]}{\det[\sigma_1 + \sigma_2]}, \tag{13}$$

$\Omega = i\hat{\sigma}_y \oplus \hat{\sigma}_y$ being the two-mode symplectic matrix, with $\hat{\sigma}_y$ one of the Pauli matrices.

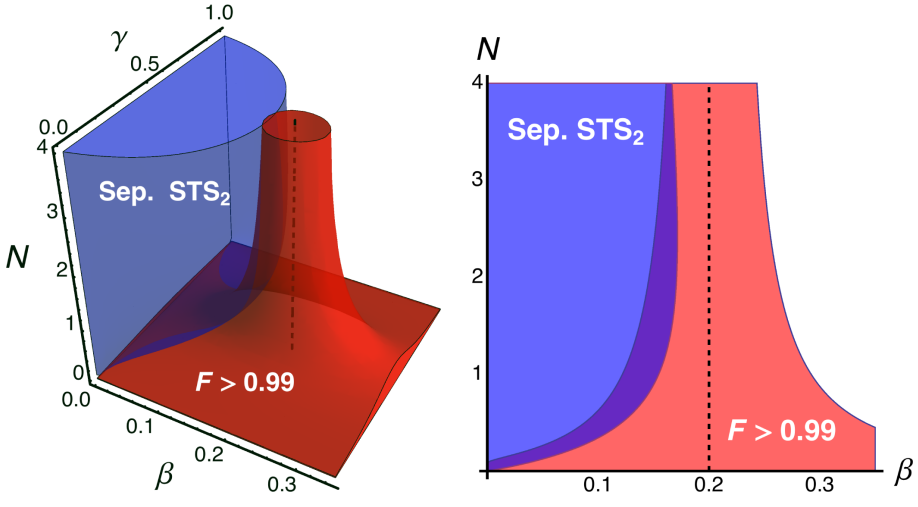

Fig. 3. (Color online) (Left panel) Separability region of STS_2 (blue region) in terms of the energy parameters N, β and γ on the left together with the volume of states having $F_{N\beta\gamma} > 0.99$ (red region) to a set of entangled target STS_2 (black-dashed line) having the same energy N with $\beta = 0.2$ and $\gamma = 0.5$. (Right panel) Section of the left panel plot in correspondence of $\gamma = 0.5$.

In the left panel of Fig. 3(a), we show the separability region in terms of the three parameters N, β and γ and the volume of states having $F_{N\beta\gamma} > 0.99$ with a set of entangled target state having the same energy N with $\beta = 0.2$ and $\gamma = 0.5$. In order to emphasize how the overlap is considerably large in the right panel we have plotted a projection on the plane where it is maximized. The region of separability is crossed by significant fraction of states over all the energy range, thus making fidelity of a little use to assess entanglement in these kind of systems though a severe constraint on the energy of the two states has been provided.

As a final example, let us consider the set of photon-number entangled states (PNES), i.e. two-mode states of the form[18,19]:

$$|\psi\rangle\rangle = \sum_n \psi_n |n, n\rangle\rangle,$$

where $|n, n\rangle\rangle \equiv |n\rangle \otimes |n\rangle$. In particular, we focus attention on two specific classes of PNES: the Gaussian two-mode squeezed vacuum states (TWB) $|\psi_T\rangle\rangle = S_2(r)|0\rangle\rangle$ and the non-Gaussian set of states resulting from the process of *photon subtraction*[20–28] applied to $|\psi_T\rangle\rangle$, i.e. $|\psi_S\rangle\rangle \propto \hat{a} \otimes \hat{b}|\psi_T\rangle\rangle$ (PSSV), where $\hat{a}$ and $\hat{b}$ are the annihilation field operators. In terms of the parameter $y = \tanh r$ we have:

$$\psi_n^T = \sqrt{1 - y^2} y^n \quad \text{and} \quad \psi_n^S = \sqrt{\frac{(1 - y^2)^3}{1 + y^2}} (1 + n) y^n, \tag{14}$$

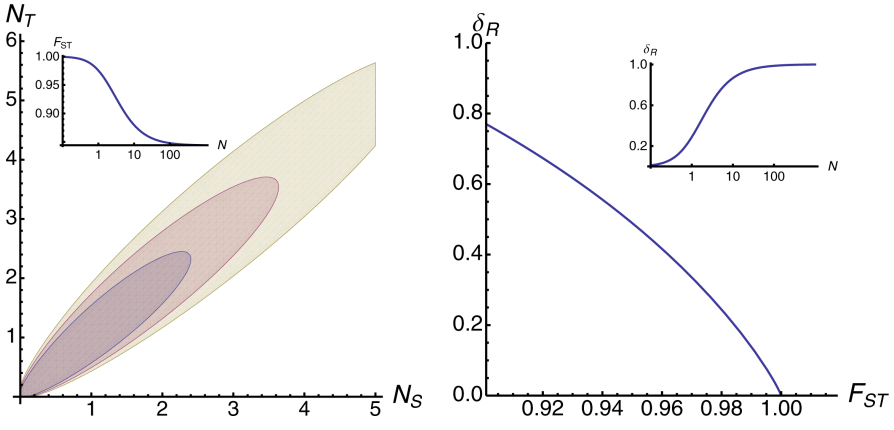

Fig. 4. (Color online) (Left panel) Regions of states having fidelity larger than 0.94, 0.92, 0.9 between a TWB and a PSSV in yellow, red and blue, respectively; in the inset the logarithmic plot of fidelity $F_{\rm ST}$ in function of the energy, with $N = N_S = N_T$, which reaches the value of $27/32$ in the limit $N \to \infty$. (Right panel) Non-Gaussianity δ_R of PSSV as a function of the $F_{\rm ST}$ to a TWB with same energy N; in the inset the logarithmic plot of δ_R in function of N.

such that the average numbers of photons are given by:

$$N_T = \frac{y^2}{1-y^2} \quad \text{and} \quad N_S = \frac{2y^2(y^2+2)}{1-y^4}. \tag{15}$$

In the left panel of Fig. 4(a), we show some region plots of the fidelity between a generic TWB and a generic PSSV

$$F_{\rm ST} = |\langle\langle \psi_S | \psi_T \rangle\rangle|^2 = \left(\sum_n \psi_n^T \psi_n^S \right)^2,$$

as a function of their average number of photons. As it is apparent from the plot, large values of fidelity, e.g. $F_{\rm ST} > 0.9$, are compatible with a relatively large range of energies, corresponding to considerably different physical properties (see below). Notice that for $N_T = N_S \equiv N$ we have $F_{\rm ST} > 27/32 \approx 0.84\ \forall N$: the inset shows the behavior of $F_{\rm ST}$ as a function of N.

A striking example of a property which cannot be assessed using fidelity is obtained by considering the non-Gaussianity of PSSV. For pure states the non-Gaussian character (quantum negentropy) of a CV states may be quantified by the Von-Neumann entropy of its reference Gaussian state, i.e. a Gaussian state with the same CM.[29–31] For PNES the non-Gaussianity $\delta[\psi]$ reduces to

$$\delta[\psi] = 2\left[\left(d_- + \frac{1}{2} \right) \log \left(d_- + \frac{1}{2} \right) - \left(d_- - \frac{1}{2} \right) \log \left(d_- - \frac{1}{2} \right) \right], \tag{16}$$

where $d_- = \sqrt{(N + \frac{1}{2})^2 - [\sum_n (1+n)\psi_n \psi_{1+n}]^2}$. The non-Gaussianity of PSSV is an increasing function of their energy. In the right panel of Fig. 4 we show the

non-Gaussianity $\delta_R[\psi_S]$ of PSSV, renormalized to its asymptotic value (in order to have $0 \leq \delta_R[\psi] \leq 1$) as a function of the fidelity F_{ST} between the PSSV and a TWB with the same energy. As it is apparent from the plot, very large values of fidelity to a Gaussian states are compatible with very large range of values of non-Gaussianity (almost the whole range). The inset shows the behavior of $\delta_R[\psi_S]$ as a function of N.

From our analysis, we conclude that also for two-mode states, fidelity should be used with caution in order to assess quantum properties, and that this remains true also when one imposes additional constraints on the energy or the squeezing fraction of the states. Notice that also in the case of two modes, full tomography[32–34] is imposing a suitable set of constraints to make fidelity a meaningful figure of merit to summarize the overall quality of the reconstruction.

4. Conclusion

In this paper we have presented several examples of single- and two-mode CV states showing that being close in the Hilbert space is by far not equivalent to share the same physical properties, e.g. quantum resources. In addition, we have shown that the phenomenon persists also when one imposes additional constraints on the energy or the squeezing of the states, thus generally questioning the use of fidelity to assess properties of CV systems. Overall, our results suggest to use fidelity only in conjunction with a tomographic set of additional constraints.

Acknowledgments

This work has been supported by MIUR through the FIRB project "LiCHIS" Nr. RBFR10YQ3H.

References

1. A. Uhlmann, *Rep. Math. Phys.* **9** (1976) 273.
2. C. M. Caves, *Phys. Rev. D* **23** (1981) 1693.
3. M. G. A. Paris, *Phys. Lett A* **201** (1995) 132.
4. U. Dorner *et al.*, *Phys. Rev. Lett.* **102** (2009) 040403.
5. C. A. Fuchs and J. van de Graaf, *IEEE Trans. Inf. Theory* **45** (1999) 1216.
6. C. Benedetti *et al.*, *Phys. Rev. A* **87** (2013) 052136.
7. V. Dodonov, *J. Phys. A* **45** (2012) 032002.
8. A. Christ, C. Lupo and C. Silberhorn, *New J. Phys.* **14** (2012) 083007.
9. M. Bina *et al.*, *Phys. Rev. A* **89** (2014) 012305.
10. C. T. Lee, *Phys. Rev. A* **44** (1991) R2775.
11. J. Twamley, *J. Phys. A* **29** (1996) 3723.
12. H. Scutaru, *J. Phys. A* **31** (1998) 3659.
13. J. Řeháček *et al.*, *Phys. Rev. A* **79** (2009) 032111.
14. H. Paul, *Rev. Mod. Phys.* **54** (1982) 1061.
15. S. Olivares, *Eur. Phys. J. ST* **203** (2012) 3.
16. Gh.-S. Paraoanu and H. Scutaru, *Phys. Rev. A* **61** (2000) 022302.
17. P. Marian and T. A. Marian, *Phys. Rev. A* **86** (2012) 022340.

18. M. Allegra, P. Giorda and M. G. A. Paris, *Phys. Rev. Lett.* **105** (2010) 100503.
19. M. Allegra, P. Giorda and M. G. A. Paris, *Int. J. Quantum Inform.* **9** (2011) 27.
20. T. Opatrný, G. Kurizki and D.-G. Welsch, *Phys. Rev. A* **61** (2000) 032302.
21. P. T. Cochrane, T. C. Ralph and G. J. Milburn, *Phys. Rev. A* **65** (2002) 062306.
22. S. Olivares, M. G. A. Paris and R. Bonifacio, *Phys. Rev. A* **67** (2003) 032314.
23. S. Olivares and M. G. A. Paris, *Phys. Rev. A* **70** (2004) 032112.
24. S. Olivares and M. G. A. Paris, *J. Opt. B* **7** (2005) 616.
25. S. Olivares and M. G. A. Paris, *Laser Phys.* **16** (2006) 1533.
26. M. S. Kim *et al.*, *Phys. Rev. A* **71** (2005) 013801.
27. J. Wenger, R. Tualle-Brouri and P. Grangier, *Phys. Rev. Lett.* **92** (2004) 153601.
28. V. Parigi *et al.*, *Science* **317** (2007) 1890.
29. M. G. Genoni, M. G. A. Paris and K. Banaszek, *Phys. Rev. A* **78** (2008) 060303(R).
30. M. G. Genoni and M. G. A. Paris, *Phys. Rev. A* **82** (2010) 052341.
31. M. G. Genoni, P. Giorda and M. G. A. Paris, *J. Phys. A* **44** (2011) 152001.
32. V. D'Auria *et al.*, *Phys. Rev. Lett.* **102** (2009) 020502.
33. D. Buono *et al.*, *J. Opt. Soc. Am. B* **27** (2010) 110.
34. R. Blandino *et al.*, *Phys. Rev. Lett.* **109** (2012) 180402.